Aircraft Performance in a JAWS Microburst

Walter Frost* and Ho-Pen Chang†
The University of Tennessee Space Institute, Tullahoma, Tennessee
and
John McCarthy‡ and Kimberly L. Elmore§
National Center for Atmospheric Research, Boulder, Colorado

A dangerous sequence of events (headwind/downdraft/tailwind) occurs when an aircraft penetrates a microburst at low levels. A prime objective of the Joint Airport Weather Studies (JAWS) project was to quantify the event so that realistic wind shear profiles would be available for computer and manned-flight simulation of aircraft performance in hazardous winds. The three-dimensional wind components of a microburst have been measured with the high-resolution dual-Doppler radars of the JAWS project conducted by the National Center for Atmospheric Research. A six-degrees-of-freedom aircraft dynamics computer program with a simple automatic control logic to simulate an aircraft flying through the microburst has been developed. Aircraft performance for 26 simulated flights through the microburst has been calculated in this paper. The flight-path deterioration parameter (FPDP) concept and the low-level wind shear alert system (LLWSAS) concept were investigated relative to the 26 simulated flights. Appraisal of the effectiveness of the FPDP and LLWSAS is given based on the simulated results. The vertical wind speed component is found to be an important parameter in the detection of hazardous wind shear. A dimensionless parameter formed from the horizontal shear of the horizontal wind speed, vertical wind speed, and height above ground is described as a possible detection signal. Correlation of this with poor flight-path control is shown. It is concluded that further analysis of the JAWS data is necessary to provide insight into the critical wind shear severity thresholds and the scales of motion that lead to dangerous aircraft responses.

Introduction

A DANGEROUS sequence of events (headwind/downdraft/tailwind) occurs when an aircraft penetrates a microburst at low levels, as illustrated in Fig. 1. If this headwind-to-tailwind reversal occurs over a short distance (1-3 km), the capability of the aircraft to negotiate the changing wind may be severely jeopardized. Figure 1 illustrates that as the aircraft approaches a microburst cell, it encounters a steadily increasing headwind which increases lift and forces the aircraft to climb above its glide slope. However, increase in drag is the result of reduced ground speed, which is not monitored for most aircraft; in fact, most pilots are unaware when ground speed, or inertial velocity, is dropping off. At the center of the microburst, the airspeed, or increasing headwind, diminishes and the aircraft encounters a strong downdraft. The downdraft velocities are much smaller near the ground than at higher altitudes because the descending air must turn and flow out horizontally. The downdraft causes a decrease in angle of attack resulting in a loss of lift. In turn, the aircraft being engulfed in the sinking air mass is carried downward. The combination of reduced lift and downdraft causes a rapid loss in altitude. If the aircraft does not impact the ground and manages to penetrate the downdraft zone, it encounters a severely increasing tailwind. The increasing tailwind further decreases the angle of attack but, more importantly, causes a significant loss of airspeed with a corresponding deterioration of aerodynamic lift. Unless the pilot immediately takes corrective action, the aircraft will impact the ground. Likewise, the same sequence of events can occur during takeoff, resulting in a performance loss that may be severe enough to cause ground impact 15-45 s after liftoff.

This paper addresses the details of a particularly severe microburst, the performance of a B-727-type aircraft as seen in a numerical simulation, and an examination of several associated low-level wind shear detection and warning concepts.

Case Study: August 5, 1982

Until recently, mathematical models of wind shear associated with microbursts had limited experimental verification and, in fact, were highly subjective. A prime objective of the Joint Airport Weather Studies (JAWS) project was to quantify the microburst wind field so that realistic three-dimensional vector wind profiles would be available for carrying out analytical and manned simulator aircraft performance studies and flight crew training.[1]

An adequate multiple Doppler radar analysis of a severe wind shear situation is required before detailed aircraft performance studies can be conducted. In this paper, a microburst event that occurred on Aug. 5, 1982 is investigated using a high-resolution dual-Doppler Analysis. After the raw Doppler data were edited to remove ground clutter at low elevation angles and velocities that had been aliased were unfolded, data were interpolated from radar space (spherical) to a Lambert conformal projection of Cartesian space using a one-pass Cressman[2] technique yielding radial velocities at regularly spaced grid points. This analysis uses an $81 \times 81 \times 9$ grid 150-m horizontal and 250-m vertical spacing representing a $12 \times 12 \times 2$ km volume in space.

A modified predictor-corrector method, using reflectivity derived hydrometer terminal fallspeed and the compressible continuity equation, is used to compute u, v, and w at each grid point. At the surface ($z = 0$ km), u and v are computed by assuming $w = 0$. Using u and v, a divergence is computed. If there are no data at the surface, u and v are estimated by assuming $w = 0$ at the first available grid level, with the resulting divergence being assumed constant from that level to the surface. Vertical velocity is then computed by integrating

Received June 4, 1984; revision received March 6, 1985.

*Director, Atmospheric Science Division; also, President, FWG Associates Inc. Tullahoma, Tenn. Member AIAA.
†Research Assistant. Member AIAA.
‡Staff Scientist. Member AIAA.
§Support Scientist. Member AIAA.

N.B.: NCAR is sponsored by the National Science Foundation.

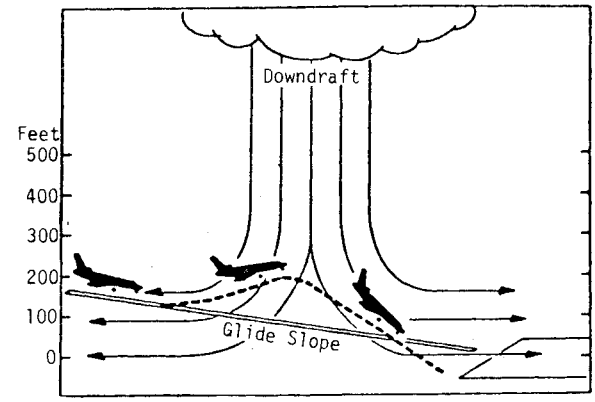

Fig. 1 Schematic of an aircraft penetration of a microburst (not to scale), indicating 1) a rapidly increasing headwind (performance increasing), 2) the remnants of the downdraft (performance decreasing), and 3) a strong tailwind (seriously decreasing performance).

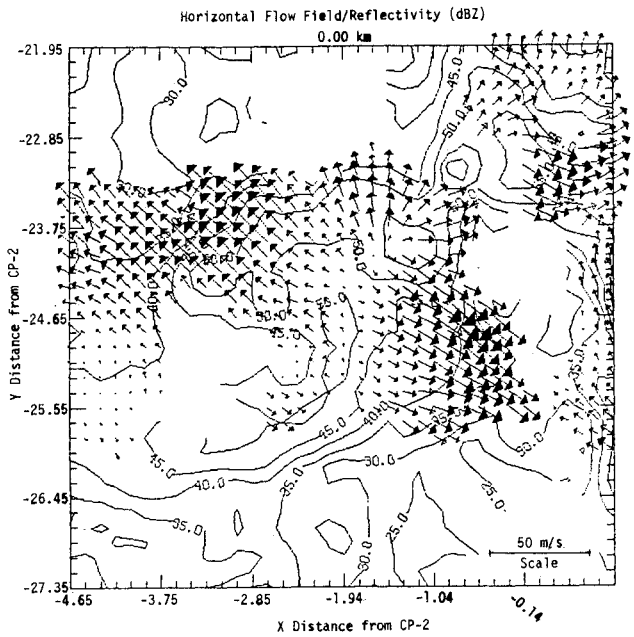

Fig. 2 Dual-Doppler radar-derived horizontal, ground-relative flowfield (scaled to the 50 m/s reference vector, upper right) and reflectivity field contours in dBZ. A 37×37 subgrid of the full 81×81 analysis is shown—distances in km.

divergence upward to the next grid level (or current grid level, if it is not at the surface), using $w=0$ at the surface as a boundary condition. Because u, v, and w are interdependent, a change in w implies a change u and v. Therefore, using the new u and v, a new divergence is computed and so on until the variation in divergence, which is a derived field and so very sensitive to changes in u and v, becomes less than a predetermined threshold. This same process is repeated for each grid level, except that w is used from the previous grid level as a first guess of w at the next higher grid level.

Figure 2 shows a horizontal plane through the ground-relative wind field near ground level centered on the principal microburst wind shear area. A strong outflow region is observed centered near (−1.6, −24.0). Figure 2 is a subgrid region of the full 81×81 analysis. A number of glide slopes or approach paths are shown superimposed upon this subregion in Fig. 3. These are not the approach paths in their entirety; they show only the most significant, lowest altitude portions of the approaches. Details of these paths are described subsequently. The vector wind field in a vertical plane through path YZ is presented in Fig. 4 as an example of the downdraft intensity. The heavy line represents that part of the approach path contained within this cross section.

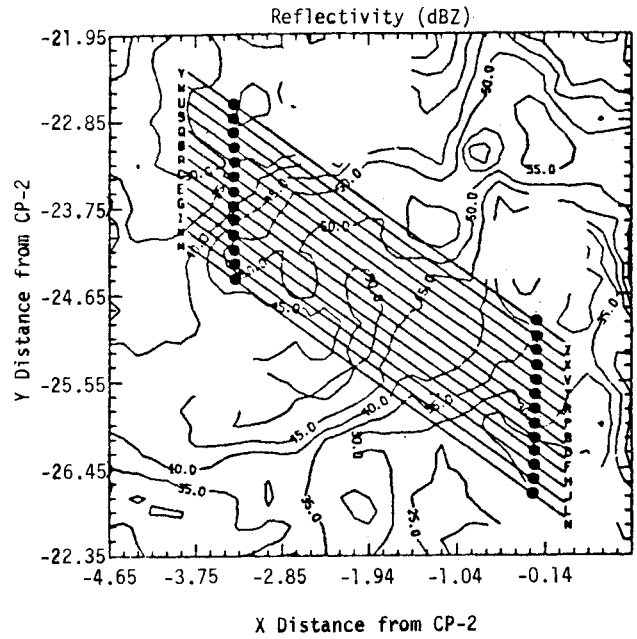

Fig. 3 Paths through the microburst along which aircraft approach simulations were performed. Black dots show intended touchdown points. Note the aircraft simulation paths extended outside the domain shown. The path segments shown encompass the most interesting part of the simulated approaches.

The three-dimensional wind field for each of the 26 simulations was input to a six-degrees-of-freedom aircraft flight dynamics computer program.¶ A volume-averaging interpolation scheme was used to interpolate data between grid points. Computer simulations of a B-727 type aircraft flying approaches from both directions along the indicated flight paths were carried out. The solid circles on the paths (Fig. 3) indicate the runway threshold (intended touchdown point). The aircraft was trimmed on a 3-deg glide slope at large distances from these points where the wind was small or essentially zero. The initial height of the aircraft was selected so that it would pass through the center of the microburst with zero wind roughly 33 m (100 ft) above the ground. Of course, the wind generally blew the aircraft off of the intended flight path and even with control inputs often missed the touchdown point.

The computer model computes flight parameters as a function of time with a numerical "pilot in the loop" who can adjust elevator, throttle settting, aileron, and rudder position according to a relatively simple control logic. These control laws are described in Ref. 3. Table 1 lists the various aerodynamic parameters investigated during the study.

Flight-Path Analysis

The computed aircraft flight-path approach-to-landing projection on the vertical (solid line) and horizontal (dashed line) planes is shown in Fig. 5 for path $\overline{ZY}$. Inspection of Fig. 5 shows that the aircraft approaching along this path from Z to Y is significantly displaced vertically from the intended path and lands roughly 1000 m short of the touchdown point. On the other hand, Fig. 6 shows that an aircraft approaching along flight path $\overline{VU}$, although experiencing some very significant departures from the flight path, is able to land within 75 m of the intended touchdown point. Interestingly, these two flight paths are displaced in the storm by a distance of only

¶Six degrees of freedom allow three components of motion to be considered: longitudinal, latitudinal, and vertical. A simpler three-degrees-of-freedom model limits the motion to longitudinal and vertical motions only.

Table 1 Aerodynamic parameters investigated along each flight path

z	Altitude along flight path
Δy	Lateral departure from runway centerline
w_x	Longitudinal wind speed component in aircraft body coordinates
w_z	Vertical wind speed component in aircraft body coordinates
w_y	Lateral wind speed component in aircraft body coordinates
$\frac{\partial w_x}{\partial x}$	Gradient in longitudinal wind speed along intended flight path
$\frac{\partial w_x}{\partial x}$	Gradient in vertical wind speed along intended flight path
$\frac{\partial w_x}{\partial x}$	Gradient in lateral wind speed along intended flight path
θ	Pitch angle
δ_E	Elevator setting
$\dot{z}$	Aircraft sink rate (inertial velocity)
ψ	Yaw angle
δ_R	Rudder setting
$\dot{y}$	Lateral ground speed (inertial velocity)
ϕ	Rolling angle
δ_a	Aileron setting
F_T	Thrust setting
V	Airspeed
$\dot{x}$	Longitudinal ground speed (inertial velocity)

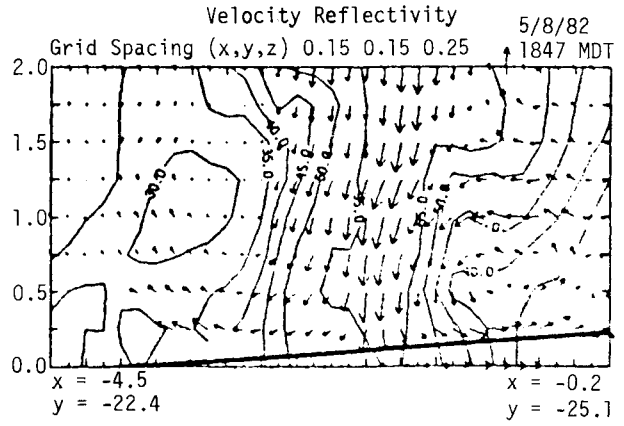

Fig. 4 Vertical cross section of dual-Doppler radar-derived winds along path $\overline{ZY}$ in Fig. 3. Flowfield vectors scaled to 15-m/s reference vector at upper right. Reflectivity contours in dBZ. Heavy dark line shows 3-deg glide slope.

300 m in the y direction. This illustrates how localized the wind shear effect is: If the storm were moving across the air field at 10 m-s^{-1}, this 300-m separation would represent only a 30-s difference between the time of the two approaches.

The wind fields encountered by the aircraft on the respective flight paths are shown in Figs. 7 and 8. One sees that an almost sinusoidal longitudinal wind speed is encountered and is approximately the same magnitude for both flight paths. In turn, the vertical velocity is similar in pattern, but the magnitude of the vertical downdraft is somewhat stronger along path $\overline{ZY}$. The cause of the significantly shorter landing along path $\overline{ZY}$ vs $\overline{VU}$ is not readily apparent by inspecting the wind speeds, although the reduced downdraft along $\overline{VU}$ may be important. This suggests examination of the higher order terms. Upon examination, the wind speed rate of change is found to strongly influence aircraft performance.

Figures 9 and 10 illustrate the wind gradients along paths $\overline{ZY}$ and $\overline{VU}$, respectively. It should be noted that, unlike the winds shown in Figs. 7 and 8, the wind gradients are not the precise wind shear encountered by the airplane. Wind field gradients along the proposed glide slope are computed from the Doppler wind field, where $\partial w_x/\partial x$, $\partial w_y/\partial x$, and $\partial w_z/\partial x$ are the longitudinal, lateral, and vertical wind shear components, respectively, along the proposed glide slope. In general, the airplane will have departed from the glide slope and will see a different wind shear. This difference, however, is expected to be small.

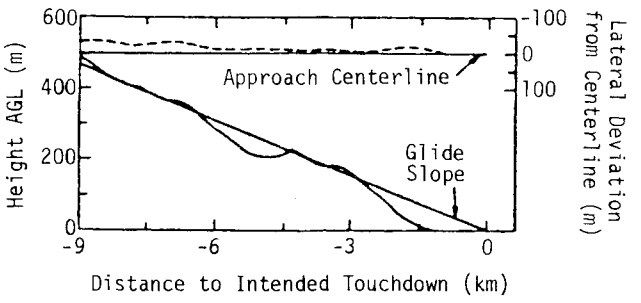

Fig. 5 Computed flight-path projections for path $\overline{ZY}$. Lateral displacement from approach centerline is given by right-hand scale. Vertical displacement from glide path is given by left-hand scale.

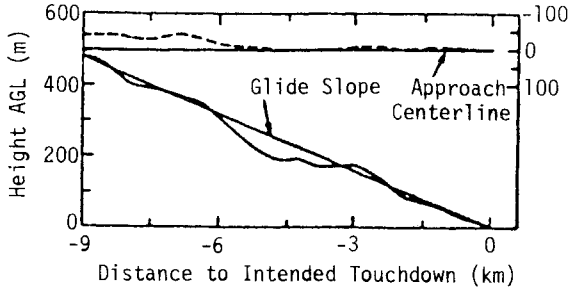

Fig. 6 The wind fields encountered by the aircraft on the respective flight paths are shown in Figs. 7 and 8. One sees that an almost sinusoidal longitudinal wind speed is encountered and is approximately the same magnitude for both flights' paths. In turn, the vertical velocity is similar in pattern, but the magnitude of the vertical downdraft is somewhat stronger along path $\overline{ZY}$. The cause of the significantly shorter landing along path $\overline{ZY}$ vs $\overline{VU}$ is not readily apparent by inspecting the wind speed, although the reduced downdraft along $\overline{VU}$ may be important. This suggests examining the higher order terms. Upon examination, the wind speed rate of change is found to strongly influence aircraft performance.

The point to be observed in the wind shear profiles in the aircraft approaching along path $\overline{ZY}$ encounters an appreciably stronger shear than the aircraft approaching along path $\overline{VU}$. This is particularly true for the variation in vertical wind, $\partial w_z/\partial x$($\sim$0.08 s^{-1} for $\overline{ZY}$ vs $\sim$0.04 s^{-1} for $\overline{VU}$), along the path but not nearly as true for longitudinal wind shears, $\partial w_x/\partial x$. Negative values of $\partial w_z/\partial x$ represent an increasing downdraft, while positive values of $\partial w_x/\partial x$ represent an increasing tailwind. Note that the aircraft encounters a relatively large shear on both approaches at a distance of approximately 4-4.5 km prior to touchdown. For a typical commercial jet airliner, this is approximately 33 s before runway contact. Considering a pilot response of approximately 3 s and an engine spool-up time of approximately 9 s, the time available for the pilot to take action to compensate for the sudden loss of aerodynamic lift associated with these gradients becomes severely limited.

Simulation of Detection and Warning Concepts

Simulations of flight in both directions along the 13 lines of flight (Fig. 3) were analyzed resulting in 26 simulated approaches. Table 2 tabulates a number of results from the analysis. Columns 1, 2, and 3 list the distance (in meters) from the intended touchdown point where the aircraft landed in each of the simulated flights. The longitudinal (Δx) and lateral (Δy) departures are presented along with the absolute value

Table 2 Computed parameters for 26 simulated flights through microburst

Flight No.	ΔX, m	ΔY, m	DD, m	N_s	LLWSAS max ΔW, m/s	σ_H, m	ΔH_A, m	ΔH_B, m	σ_V, m/s	Δ_{V_A}, m/s	Δ_{V_B}, m/s
NM	125.8	−2.2	125.8	0.0001	8.5	4.69	1.07	0.99	1.19	0.40	−1.10
LK	34.2	2.6	34.3	0.0244	10.0	5.76	1.11	0.95	1.94	0.69	−1.86
JI	130.1	7.1	130.3	0.0079	13.3	5.62	1.09	0.96	2.77	1.15	−2.35
HG	764.2	−5.7	764.2	0.0079	16.8	11.20	1.11	0.93	3.56	1.64	−3.07
FE	−228.4	14.6	228.9	0.0197	15.8	12.60	1.11	0.85	4.21	2.12	−3.70
DC	125.3	33.0	129.6	0.0205	13.3	16.20	1.13	0.74	5.02	2.91	−4.00
BA	126.9	26.0	129.6	0.0169	14.9	19.50	1.09	0.63	5.72	3.43	−4.58
PO	56.8	−21.2	60.6	0.0202	16.7	22.70	1.13	0.59	6.11	3.82	−4.77
RQ	129.5	−8.4	129.8	0.0258	16.2	23.90	1.11	0.58	6.24	3.98	−4.83
TS	−411.7	2.3	411.7	0.0331	15.4	24.10	1.16	0.63	6.17	3.82	−5.01
VU	56.5	−0.2	56.5	0.0502	14.9	24.90	1.27	0.67	6.15	3.73	−5.24
XW	−471.6	4.1	471.7	0.0831	14.0	25.30	1.18	0.67	6.20	3.70	−5.40
ZY	−1050.7	6.9	1050.8	0.1136	12.7	22.80	1.46	0.78	6.06	3.61	−5.55
YZ	−566.5	−2.4	566.5	0.1127	18.3	10.40	1.11	0.99	2.89	1.98	−2.30
WX	−478.1	−3.2	478.1	0.0739	18.9	9.52	1.11	0.98	2.79	1.99	−1.96
UV	56.5	−0.22	56.5	0.0502	17.0	9.61	1.13	0.99	3.24	2.37	−2.13
ST	−70.0	3.1	70.0	0.0307	15.6	11.60	1.16	0.98	3.19	2.43	−2.15
QR	180.7	4.4	180.7	0.0237	18.5	11.70	1.17	0.98	3.34	2.61	−2.18
OP	209.4	18.6	210.2	0.0207	16.0	12.10	1.24	0.98	3.30	2.40	−2.15
AB	226.4	13.4	226.8	0.0194	10.5	11.60	1.24	0.99	3.36	2.43	−2.05
CD	−36.3	9.7	37.5	0.0199	8.3	11.20	1.18	0.99	3.40	2.30	−2.11
EF	−19.5	20.2	28.0	0.0187	8.0	10.90	1.15	0.99	3.29	2.40	−1.92
GH	96.8	6.5	97.0	0.0233	8.3	10.00	1.21	0.99	3.25	2.36	−1.88
IJ	0.9	0.3	1.0	0.0123	8.4	10.50	1.21	0.99	2.98	2.17	−1.60
KL	76.8	1.9	76.8	0.0040	7.9	10.30	1.59	0.99	2.36	1.56	−1.41
MN	−322.7	0.2	322.7	0.0064	8.1	6.69	1.13	1.00	1.50	1.09	−0.93

$DD = \sqrt{\Delta x^2 + \Delta y^2}$. A negative departure in the horizontal direction corresponds to landing short of the intended touchdown point, and a negative value in the lateral direction represents landing to the left. The computed results for each approach cannot be construed as the only possible outcome of the flight. For any given wind condition, the actual flight path would depend on the pilot and/or automatic control laws, as well as several other factors. The computed results of the 26 simulated flight paths, however, are consistent among themselves and do provide a good comparative measure of the severity of wind shear along the particular path of interest. It is observed from Table 2 that 10 of the flights landed 200 m or more outside the intended touchdown point. Of these, eight landed short, whereas two landed long.

The results of the 26 simulated flights were studied relative to hazard definitions and to two detection and warning concepts. The flight-path deterioration parameter (FPDP) concept reported by Frost,[4] Turkel et al.,[3] and McCarthy et al.,[5] and the low-level wind shear alert system (LLWSAS) concept reported by Goff[6] were investigated.

The LLWSAS is currently installed at some 59 airports (an additional 61 airports will be included by 1985) and consists of five peripheral anemometers distributed around the airport at a radius of ≈3 km from a centerfield site. When the vector difference in wind velocity equals or exceeds 7.5 m-s^{-1} (15 knots) between the central anemometer and any one of the peripheral anemometers, a warning is sounded in the control tower. In the current analytical study, the simulated positions of the peripheral anemometers were on a 2400-m radius from the touchdown point. Five anemometers located at stations north, northwest, northeast, southwest, and southeast were simulated. The central anemometer was assumed to be at the touchdown point. Note that, in the simulation, the vector differences are taken between winds measured essentially simultaneously. The actual LLWSAS's use a 2-min averaged central wind and 10-s averaged peripheral winds, which severely limit the central anemometer's ability to detect the short-term wind variations that characterize microbursts.

The maximum vector difference sensed by the LLWSAS for each flight is tabulated in Table 2. Because the LLWSAS sounds an alarm at 7.5 m-s^{-1} (15 knots) or greater, the simulation indicates that an alarm would have sounded for all of the cases analyzed. Further inspection of the table shows no apparent correlation between the magnitude of the LLWSAS signal with that of the departure from touchdown, DD.

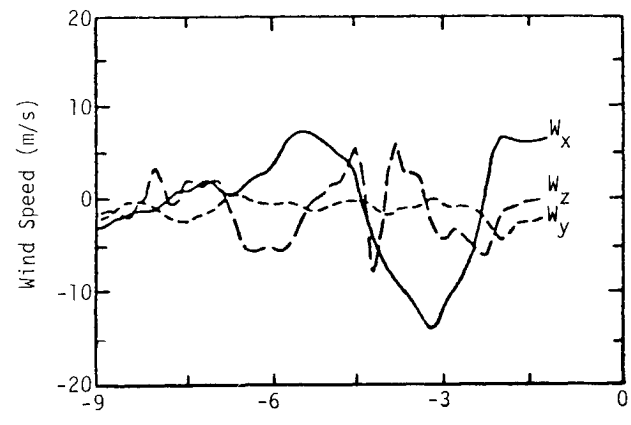

Fig. 7 Wind speed components encountered by aircraft along path ZY. W_x is the longitudinal component, W_y the lateral component, W_2 and the vertical component.

A Doppler radar pointed along the approach path measures the wind speed. A computer "Slaved" to the radar computes the aircraft performance essentially in real time with a simple aircraft dynamic algorithm and displays a FPDP value in the control tower. The value of the FPDP is a measure of the departure of the aircraft from its intended flight conditions, and thus is the degree of hazard associated with the prevailing winds. A major effort of the aircraft performance study with the JAWS data sets is to define a meaningful FPDP, to establish a value indicative of hazardous conditions, and to determine the necessary radar scanning strategies for reliably computing the value in real time.

The initial FPDP concept called for the Doppler radar beam to be fixed along the 3 deg approach and departure paths. With this procedure, only the longitudinal component (i.e.,

Table 3 Definition of flight deterioration parameters used in simulation evaluation

$$\sigma_H = \sqrt{\frac{1}{T_L}\int_0^{T_L}(HP-HG)^2 dt}$$

where T_L is total landing time, HP the aircraft altitude, and HG the glide slope height.

$$\Delta H_A = \frac{1}{T_n}\int_0^{T_n}\frac{HP}{HG}dt$$

where HP/HG is above or on glide slope ≥ 1 and T_n is the time above or on glide slope. T_n/T_L is the percentage of time above or on glide slope.

$$\Delta H_B = \frac{1}{T_m}\int_0^{T_m}\frac{HP}{HG}dt$$

where HP/HG is below glide slope < 1 and T_m is the time below glide slope. T_m/T_L is the percentage of time below glide slope.

$$\sigma_V = \sqrt{\frac{1}{T_L}\int_0^{T_L}(V_a - V_{a_0})^2 dt}$$

where V_a is the airspeed and V_{a_0} the reference airspeed.

$$\Delta V_A = \frac{1}{T_i}\int_0^{T_i}(V_a - V_{a_0})dt$$

for $V_a - V_{a_0} \geq 0$, where T_i is the time the airspeed is equal to or greater than reference airspeed. T_i/T_L is the percentage of time above or equal to the reference airspeed.

$$\Delta V_B = \frac{1}{T_k}\int_0^{T_k}(V_a - V_{a_0})dt$$

for $V_a - V_{a_0} < 0$, where T_k is the time the airspeed is below the reference airspeed. T_k/T_L is the percentage of time below the reference airspeed.

radial component) of the wind velocity is measured. At small elevation angles the radar return is relatively insensitive to vertical winds.

Six definitions of possible FPDP's given in Table 3 were calculated along each flight path. These values are tabulated in Table 2. The flight deterioration parameter represents departures or variations of altitude and airspeed from nominal values along the flight path. They are based, however, on the assumption that the airplane encounters only the radial velocity component; in actual flight the aircraft encounters all three wind velocity components. Note that the aircraft will not only experience the additional vertical and lateral wind components that are not measured by the radar, but will also experience different longitudinal winds if it departs appreciably from the path viewed by the radar.

The purpose of the simulation described above was to determine whether a detection and warning system based on this concept could detect those wind shear conditions that are nonnegotiable by the aircraft. However, no clear correlation between any of the FPDP values tabulated in Table 2 and DD is evident. DD is a measure of impact with the ground outside the intended touchdown point. It is quite possible that this poor correlation is due to the inherent lack of vertical and lateral wind components.

Figure 11 compares the flight paths along $\overline{ZY}$ and $\overline{VU}$ computed with the simplified three-degrees-of-freedom model for the aircraft and with the simulated radar-measured winds. The aircraft follows essentially the same flight path for both glide slopes and drastically overshoots the touchdown point in each case. Figure 12 is a plot of the winds experienced during each

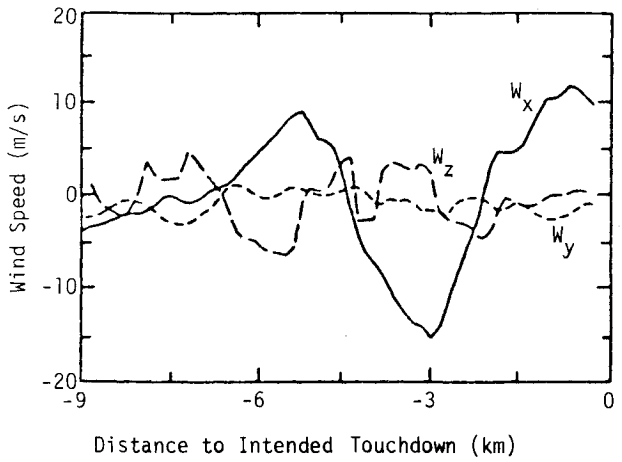

Fig. 8 Same as Fig. 7 but for path $\overline{VU}$.

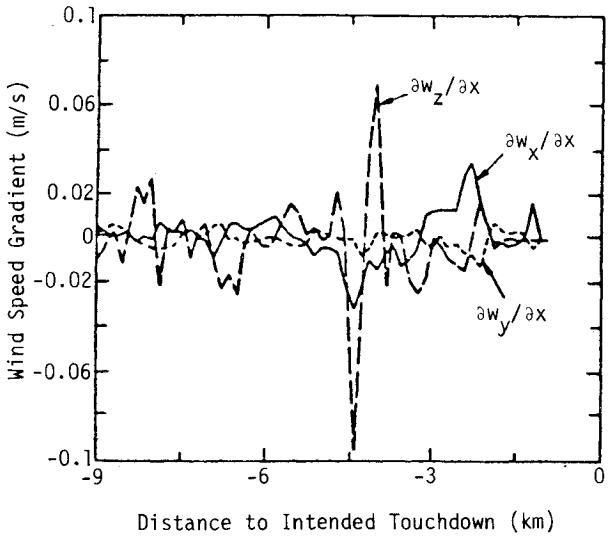

Fig. 9 Longitudinal wind speed gradients encountered by aircraft along path $\overline{ZY}$. $\partial w_x/\partial x$ is the longitudinal gradient of the longitudinal component, $\partial w_y/\partial x$ the longitudinal gradient of the lateral component, and $\partial w_z/\partial x$ the longitudinal gradient of the vertical component.

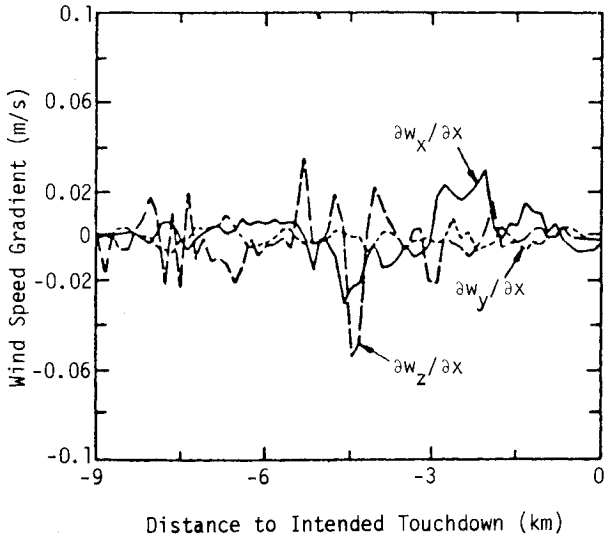

Fig. 10 Same as Fig. 9 but for path $\overline{VU}$.

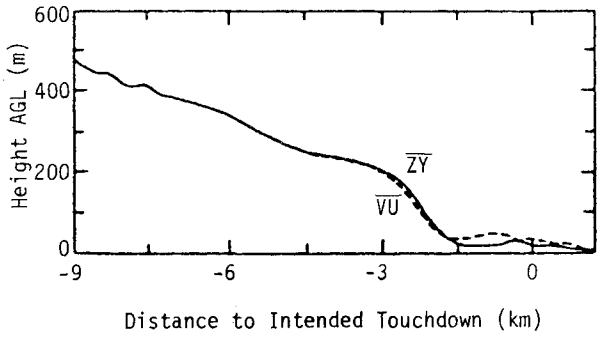

Fig. 11 Computed flight-path projections on vertical plane using a simplified three-degrees-of-freedom aircraft dynamics model. Model input data are the single Doppler winds from Fig. 12.

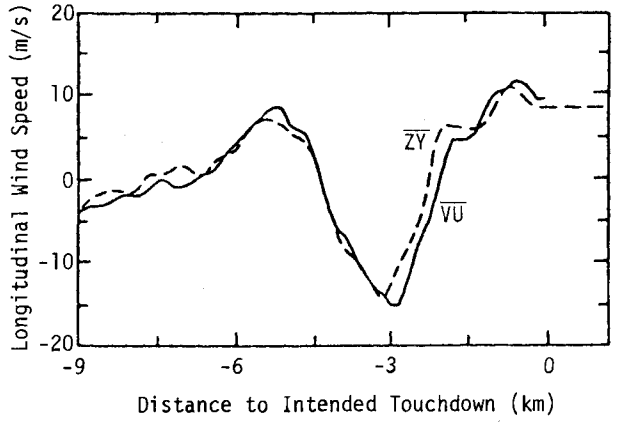

Fig. 12 Single Doppler longitudinal wind speeds measured along glide slopes $\overline{VU}$ and $\overline{ZY}$ by a radar at the intended touchdown points.

approach as measured by the Doppler radar. The wind speed at horizontal positions $x>0$ remains constant because the radar is assumed to be located at the touchdown point, and does not measure winds past that point. Comparison of these winds with the longitudinal components shown in Figs. 7 and 8 shows very little difference. Consequently, at least in terms of characterizing aircraft performance in this sort of wind shear condition, the longitudinal component does not provide the necessary precision.

Examination of the data from this study clearly indicates that three factors cause large values of DD. These factors are: 1) positive values of $\partial w_x/\partial x$ (headwind shearing to tailwind), 2) negative values of w_z (downdraft), and 3) small values of z (the height above the ground) from which these wind effects are encountered. A dimensional number (in units of s^{-2}) defined as $N_s = w_z(\partial w_x/\partial x)/z$ was computed for each flight path and the maximum value along each flight path was tabulated (Table 2, column 4). Values of N_s are plotted vs the horizontal touchdown departure (Δx) in Fig. 13. With the exception of one outlying value, the correlation appears reasonably valid considering all of the parameters involved. This simple correlation suggests that a detection and warning system which provides a realistic estimate of aircraft hazard in a (microburst) wind shear situation, should monitor the three parameters making up N_s along the flight path. Methods of achieving this with Doppler radar in the terminal airport area are not obvious without utilizing a dual-Doppler radar system. However, the three-dimensional wind fields resulting from JAWS provide meaningful data sets from which a detailed conceptual development of detection and warning techniques can be carried out through computer simulations.

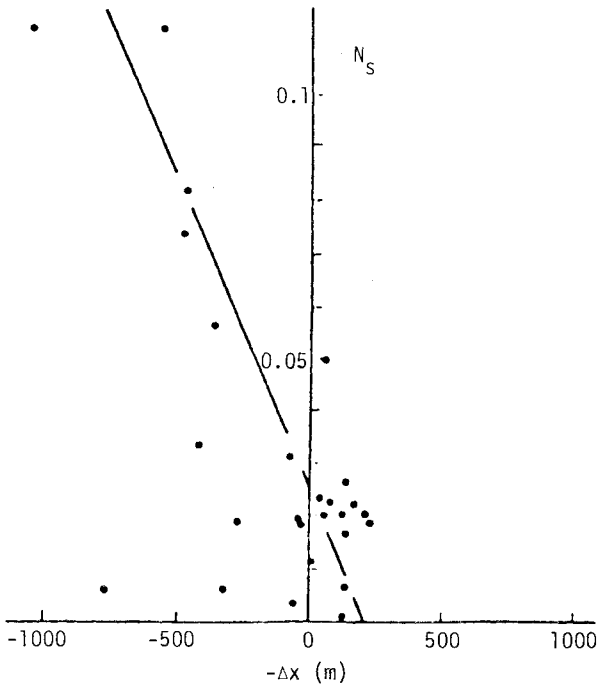

Fig. 13 Scatter diagram showing the shear parameter N_s vs the computed approach undershoot or overshoot magnitude.

Conclusions

A wealth of knowledge relative to the investigation of aircraft performance in hazardous wind shear is contained in the Joint Airport Weather Studies (JAWS) data sets. This paper demonstrates how three-dimensional vector wind fields can be incorporated into aircraft dynamics models and how the calculation of meaningful flight paths can be carried out effectively under varying wind conditions. Clearly, this utility of the JAWS data leads to assurance of its compatibility with algorithms for driving manned flight simulators in which training and research investigations can be informed.

In addition, testing of wind shear detection and warning system performance in experimentally established, three-dimensional vector wind fields, and comparison of the results with computed aircraft performance provide a viable technique for verifying the concept and establishing design criteria for developing these systems.

Simulation of a simple flight-path deterioration parameter (FPDP) concept was carried out. The radial wind speed component that would be sensed by a radar, fixed to look along the glide slope, was used as input to an aircraft dynamics computer program. Values of FPDP's calculated from this simulation indicated limited if no correlation with poor aircraft touchdown performance. This is not overly surprising, since the FPDP technique tested is a simple initial concept. A dimensional parameter N_s (which includes the effects of a downdraft, a headwind-to-tailwind shear, and the height above ground level at which this effect occurs) shows reasonable correlation with the computed magnitudes of departure from touchdown. A conclusion from these results, however, suggests that the vertical, as well as the longitudinal wind component, should be considered to precisely characterize aircraft performance. The radial, or longitudinal, wind component, can be measured clearly by an airport Doppler radar situated near the runway. Even though the latitudinal and vertical wind components are unavailable with this technique, strongly diverging flow near the surface (which can be detected by an airport Doppler radar) is sufficiently dangerous to keep aircraft away from the shear region. Furthermore, diverging outflow near the surface must be at the base of a strong downdraft. In other words, because the

shear conditions are so variable in space and time as demonstrated by these simulations, a Doppler-based detection and warning system should not attempt to supply the high precision required by an aircraft to thread its way through such a shear. Instead, the presence of any strong (horizontal) wind shear provides sufficient guidance for the aviation system to avoid it. Consequently, a viable detection and warning system could be established without measuring the latitudinal and vertical wind components directly. Additional details on the airport Doppler concept can be found in Ref. 7.

A simplified simulation of the low-level wind shear alert system (LLWSAS) indicated that an alarm would have sounded for each flight path investigated. Although many of these flight paths concluded with a successful touchdown, one should not necessarily assume that the LLWSAS produced numerous false alarms. Bear in mind that even those flight paths that did not end in a short touchdown and had high impact were, by any standards, still difficult to negotiate. Thus, from a safety point of view, an aircraft arriving at the simulated airport should, in fact, wait until the microburst moves away or dissipates.

Further analysis of the JAWS data is being carried out to provide insight into critical wind shear severity thresholds, the scales of motion that lead to dangerous aircraft response, the relative importance of horizontal vs vertical wind speed components, the definition and methods of testing flight deterioration parameters, and the evaluation of operational procedures for use in wind shear encounters.

Acknowledgments

The dual-Doppler program used in this study runs on the NCAR Atmospheric Technology Division's VAX 11/780. It was modified and implemented at NCAR by Ms. Cathy Kessinger of the JAWS staff and was originally developed by Dr. Peter S. Ray and Mr. Conrad L. Ziegler at NOAA's National Severe Storms Laboratory in Norman, Oklahoma.

This work is partially funded by NCAR Subcontract S3011 to FWG Associates Inc. JAWS is funded partially by NCAR; the National Science Foundation; the FAA, through Interagency Agreement DTFA01-82-Y-10513; and NOAA, through a cooperative agreement with the Program for Regional Observing and Forecasting Services of NOAA's Environmental Research Laboratory.

References

[1]McCarthy, J., Wilson, J. W., and Fujita, T. T., "The Joint Airport Weather Studies Project," *Bulletin of the American Meteorological Society*, Vol. 63, 1982, pp. 15-22.

[2]Cressman, G. P., "An Operational Objective Analysis System," *Monthly Weather Review*, Vol. 87, 1959, pp. 367-374.

[3]Turkel, B. S., Kessel, P. A., and Frost, W., "Feasibility Study of a Procedure to Detect and Warn of Low-Level Wind Shear," NASA CR 3480, 1981.

[4]Frost, W., "Flight in Low-Level Wind Shear," NASA CR 3678, 1983.

[5]McCarthy, J., Blick, E. F., and Elmore, K. L., "An Airport Wind Shear Detection and Warning System Using Doppler Radar—A Feasibility Study," NASA CR 3379, 1981.

[6]Goff, R. C., "The Low-Level Wind Shear Alert System (LLWSAS)," Federal Aviation Administration, Washington, D. C., FAA-RD-80-45, 1980.

[7]Wilson, J. W. and Roberts, R. D., "Evaluation of Doppler Radar for Airport Wind Shear Detection," *Preprints, 21st Radar Meteorological Conference*, Edmonton, Alberta, Canada, American Meteorological Society, 1983.